The EMBO Journal (2006) 25, 3943–3954 | © 2006 European Molecular Biology Organization | All Rights Reserved 0261-4189/06
www.embojournal.org

THE EMBO JOURNAL

Direct binding of p85 to sst2 somatostatin receptor reveals a novel mechanism for inhibiting PI3K pathway

Corinne Bousquet[1,4,*], Julie Guillermet-Guibert[1,4], Nathalie Saint-Laurent[1], Elodie Archer-Lahlou[1], Frédéric Lopez[2], Marjorie Fanjul[1], Audrey Ferrand[1], Daniel Fourmy[1], Carole Pichereaux[3], Bernard Monsarrat[3], Lucien Pradayrol[1], Jean-Pierre Estève[1] and Christiane Susini[1]

[1]INSERM U531, Institut Louis Bugnard, CHU Rangueil, Toulouse cedex 4, France, [2]IFR 31, Institut Louis Bugnard, CHU Rangueil, Toulouse cedex 4, France and [3]Institut de Pharmacologie et de Biologie Structurale, CNRS, Toulouse cedex, France

Phosphatidylinositol 3-kinase (PI3K) regulates many cellular functions including growth and survival, and its excessive activation is a hallmark of cancer. Somatostatin, acting through its G protein-coupled receptor (GPCR) sst2, has potent proapoptotic and anti-invasive activities on normal and cancer cells. Here, we report a novel mechanism for inhibiting PI3K activity. Somatostatin, acting through sst2, inhibits PI3K activity by disrupting a pre-existing complex comprising the sst2 receptor and the p85 PI3K regulatory subunit. Surface plasmon resonance and molecular modeling identified the phosphorylated-Y^{71} residue of a p85-binding pYXXM motif in the first sst2 intracellular loop, and p85 COOH-terminal SH2 as direct interacting domains. Somatostatin-mediated dissociation of this complex as well as p85 tyrosine dephosphorylation correlates with sst2 tyrosine dephosphorylation on the Y^{71} residue. Mutating sst2-Y^{71} disabled sst2 to interact with p85 and somatostatin to inhibit PI3K, consequently abrogating sst2's ability to suppress cell survival and tumor growth. These results provide the first demonstration of a physical interaction between a GPCR and p85, revealing a novel mechanism for negative regulation by ligand-activated GPCR of PI3K-dependent survival pathways, which may be an important molecular target for antineoplastic therapy.

The EMBO Journal (2006) **25,** 3943–3954. doi:10.1038/sj.emboj.7601279; Published online 17 August 2006
Subject Categories: signal transduction; molecular biology of disease
Keywords: cell survival; G protein-coupled sst2 somatostatin receptor; PI3K pathway; protein interaction; tumor growth

*Corresponding author. INSERM U531, IFR31, Institut Louis Bugnard, BP 84225, CHU Rangueil, 31432 Toulouse cedex 4, France.
Tel.: +33 5 61 32 24 07; Fax: +33 5 61 32 24 03;
E-mail: Corinne.Bousquet@toulouse.inserm.fr.
[4]These authors contributed equally to this work

Received: 11 November 2005; accepted: 21 July 2006; published online: 17 August 2006

Introduction

The balance between cell survival and cell death critically controls tissue homeostasis. Growth factors, cytokines and integrins regulate this balance by activating Class I_A phosphatidylinositol 3-kinase (PI3K) and excessive activation of this enzyme is a hallmark of a wide range of tumors (Vivanco and Sawyers, 2002; Luo *et al*, 2003). Class I_A PI3K is a heterodimer consisting of a regulatory subunit (p85) and a catalytic subunit (p110), which catalyzes phosphorylation of phosphatidylinositol (PtdIns)-4,5-P_2 to PtdIns-3,4,5-P_3. These lipids recruit the proteine kinase Akt to the plasma membrane by engaging its PH domain, an event that triggers phosphorylation and activation of Akt. PI3K regulates a diverse array of cellular functions including cell survival, growth, proliferation, intermediary metabolism and cytoskeletal rearrangements (Cantley, 2002; Vivanco and Sawyers, 2002). Physical interaction of p85 SH2 domain with tyrosine-phosphorylated molecules, in the context of a YXXM consensus motif present in either activated tyrosine kinase receptors or their adapter molecules, and phosphorylation of p85 Tyr688 are directly responsible for ligand-induced PI3K regulation (Cuevas *et al*, 2001; Chan *et al*, 2002). p85 also interacts directly with the ion channel NMDA receptor (Takagi *et al*, 2003), as well as with estrogen and glucocorticoid receptors (Simoncini *et al*, 2000; Leis *et al*, 2004), resulting in ligand-inducible PI3K regulation. In contrast, although several ligand-activated GPCR, including gastrin, or the angiotensin AT2 receptor, regulate PI3K activity (Daulhac *et al*, 1999; Cui *et al*, 2002), no physical interaction has been demonstrated to occur between these receptors and p85, but rather with receptor-activated signaling molecules.

A range of mechanisms is involved in negative regulation of PI3K activity in response to growth factors. For example, dephosphorylation of p85 on Tyr688 by the tyrosine phosphatases SHP-1, or phosphorylation on Ser608 by the intrinsic protein kinase activity of the p110 catalytic subunit inhibits PI3K activity (Cuevas *et al*, 1999; Foukas *et al*, 2004). The tyrosine phosphatase SHP-2 negatively regulates some growth factor-induced PI3K activation by dephosphorylating p85-binding sites on Gab-1 (Zhang *et al*, 2002). Another negative feedback inhibition of insulin-induced PI3K activation might involve mTOR signaling, which affects IRS-1 phosphorylation and transcription (Harrington *et al*, 2005).

The inhibitory GPCR sst2 receptor transduces somatostatin antiproliferative, apoptotic, antiangiogenic and anti-invasive effects (Weckbecker *et al*, 2003; Bousquet *et al*, 2004). Interestingly, sst2 behaves as a tumor suppressor gene for pancreatic cancer. A selective sst2 loss is observed in 90% of human pancreatic adenocarcinomas (Buscail *et al*, 1996). Re-expression of sst2 in human pancreatic cancer cells results both in increased apoptosis and cell-sensitization to death ligand-induced apoptosis (Guillermet *et al*, 2003), and

in decreased pancreatic cancer cell proliferation and tumorigenicity (Vernejoul *et al*, 2002; Kumar *et al*, 2004).

Here, we report a novel mechanism for limiting PI3K activity. We present evidence for the first time for a physical interaction between a GPCR, sst2 and the PI3K regulatory subunit p85, occurring through the tyrosine-phosphorylated Y^{71}AKM sequence, present in the sst2 first intracellular loop (il_1). Interestingly, the somatostatin analog RC-160 inhibits PI3K activity by disrupting sst2–p85 complexes, triggering inhibition of cell survival and tumor growth. This observation is of interest as excess activation of the PI3K pathway has been reported in pancreatic adenocarcinomas (Asano *et al*, 2004), and potently participates in the acquisition of both an invasive phenotype and resistance of pancreatic cancer cells to chemotherapy (Ng *et al*, 2000).

Results and discussion

The regulatory subunit p85 of PI3K directly interacts with the sst2 phosphorylated-Y^{71} residue

To identify novel sst2 interacting partners, sst2 protein sequence was screened and a consensus YXXM motif, known to bind the PI3K regulatory p85 subunit when the Y residue is phosphorylated, was identified in sst2-il_1 (sequence Y^{71}AKM^{74}). We therefore investigated by surface plasmon resonance (SPR) for a direct interaction between p85 and sst2. A recombinant GST-p85 protein was shown to directly and specifically interact with a peptide, encompassing the sst2-il_1 sequence and immobilized on the chip, only when the residue Y^{71} is phosphorylated (pY^{71}-peptide), yielding a differential response (see Materials and methods) increasing with the concentration of the injected GST-p85 (Figure 1A). The calculated K_D was 16 nM. Endogenous p85 was then shown to specifically interact with the pY^{71}-peptide, as demonstrated by the subsequent injection of a cell extract resulting in a significant differential response on the sst2-il_1-pY^{71}-peptide, which was further increased after injecting an anti-p85 antibody, but not unrelated antibodies (Figure 1B).

Strikingly, mass spectrometry (MS) analysis coupled with SPR successfully identified p85, recovered from binding to the sst2-il_1 pY^{71}-peptide of proteins derived from the injection of a p85-transfected cell extract, as interacting with sst2 with a 27% sequence covering (Supplementary Figure 1). This result validates this promising approach to uncover novel protein interacting partners.

Mutation of the Y residue included in the consensus YXXM motif, whereby Y is phosphorylated, is known to block p85 interaction with this motif (Vivanco and Sawyers, 2002). To investigate whether wild-type but not mutated Y^{71}F sst2 might interact with p85, a recombinant GST-p85 protein was immobilized onto the chip to serve as a bait, and either mock-, wild-type or mutated Y^{71}F flag-tagged sst2-transfected cell extracts were injected (Figure 1C, left, middle or right panel, respectively). Among the proteins of the cell extracts that bind GST-p85, sst2 was identified specifically in the wild-type sst2-tranfected cell extract, as indicated by the further increase in the differential response observed in the wild-type (middle panel, plain line), but not mock or mutated Y^{71}F sst2 conditions (left or right panels, respectively, plain lines), after injecting the anti-flag antibody. This anti-flag antibody-mediated response, observed in the presence of wild-type sst2, was however abrogated when a competitive concentration of the pY^{71}-peptide was coinjected with the cell extract (middle panel, dotted line), whereas no effect was observed with mock or mutated Y^{71} sst2-expressing cell extracts. This result indicated that sst2 interaction with GST-p85 was displaced by using an excess of the sst2-il_1-pY^{71}-peptide.

Finally, a pull-down experiment was performed to further confirm the sst2–p85 interaction (Figure 1D). Consistently, sst2 was recovered in the pull-down experiment using GST-p85 and wild-type sst2-expressing cell extract, but not in the presence of GST alone, or when mock or mutated Y^{71}F sst2-transfected cell extracts were used. When compared to the total input of wild-type sst2-expressing cell extract, about 5% of sst2 was bound to GST-p85. These results establish that GST-p85 was able to recover sst2 as a binding partner in cell extracts, indicating that both full-length proteins interact effectively. These data also convincingly suggest that the phosphorylated status of the sst2-Y^{71} residue is a prerequisite for sst2 and p85 to interact.

To validate our experimental results, we designed a molecular model for the sst2–p85 interaction by docking sst2-il_1 and p85 C- or N-terminal SH2 domain (SH2c or SH2n). We hypothesized that a p85 SH2 domain is involved in the interaction, as suggested by the requirement for the sst2-pY^{71} residue. Both p85-SH2c and SH2n domains have similar specificity to the sequence context of pY-hydrophobic-X-hydrophobic, in accordance with $pY+1$ being an alanine and $pY+3$ a methionine in sst2-il_1 (Vivanco and Sawyers, 2002). p85-SH2n domain was demonstrated not to be involved in the sst2–p85 interaction, as no interaction occurred between sst2-il_1 and a recombinant GST-p85-SH2n by SPR (not shown). By contrast, docking p85-SH2c to sst2-il_1 yielded a refined model of this complex whereby sst2-il_1 is located in a groove of the p85-SH2c (Supplementary Figure 2A). Accordingly, pY^{71} is inserted deeper into a binding pocket through robust interactions between its phosphate group and p85-SH2c residues E^{635} and R^{649}. Interestingly, sst2 R^{70} and K^{75} residues appeared also involved in the interaction with p85-SH2c, through hydrogen bonds with E^{635} and E^{666}, and D^{708}, respectively (Supplementary Figure 2B). According to the model, full-size recombinant GST-p85 proteins containing single or multiple mutations on these p85-SH2c residues (E^{635}L, R^{649}M, E^{666}L and D^{708}A) were tested using SPR and the Y^{71}-containing sst2-il_1 peptides, either phosphorylated or not (Supplementary Figure 2C). Single mutations of p85-SH2c R^{649}, but not of E^{635}, E^{666} or D^{708}, abrogated the sst2–p85 interaction. Consistently, R^{649} is included in the p85-SH2c FLVR motif, which is critical for SH2 domains to interact with phosphotyrosine (Kuriyan and Cowburn, 1997). Mutations of the three E^{635}, E^{666} and D^{708} residues together decreased the sst2–p85 interaction by 50%, suggesting that their interactions with sst2 R^{70} and K^{75} residues stabilize the complex. Preferential interaction of p85-SH2c, rather than p85-SH2n, with phosphotyrosine residues was also demonstrated for NMDA (Takagi *et al*, 2003) or PDGF receptor (Panayotou *et al*, 1993).

Sst2 co-immunoprecipitates in cells with p85 and with a PI3K activity

To assess whether sst2 and p85 interact within a cellular context, wild-type or mutated Y^{71}F flag-tagged sst2 was transfected together with HA-tagged p85 in COS-7 cells (Figure 2A). In basal conditions (in the presence of serum without addition

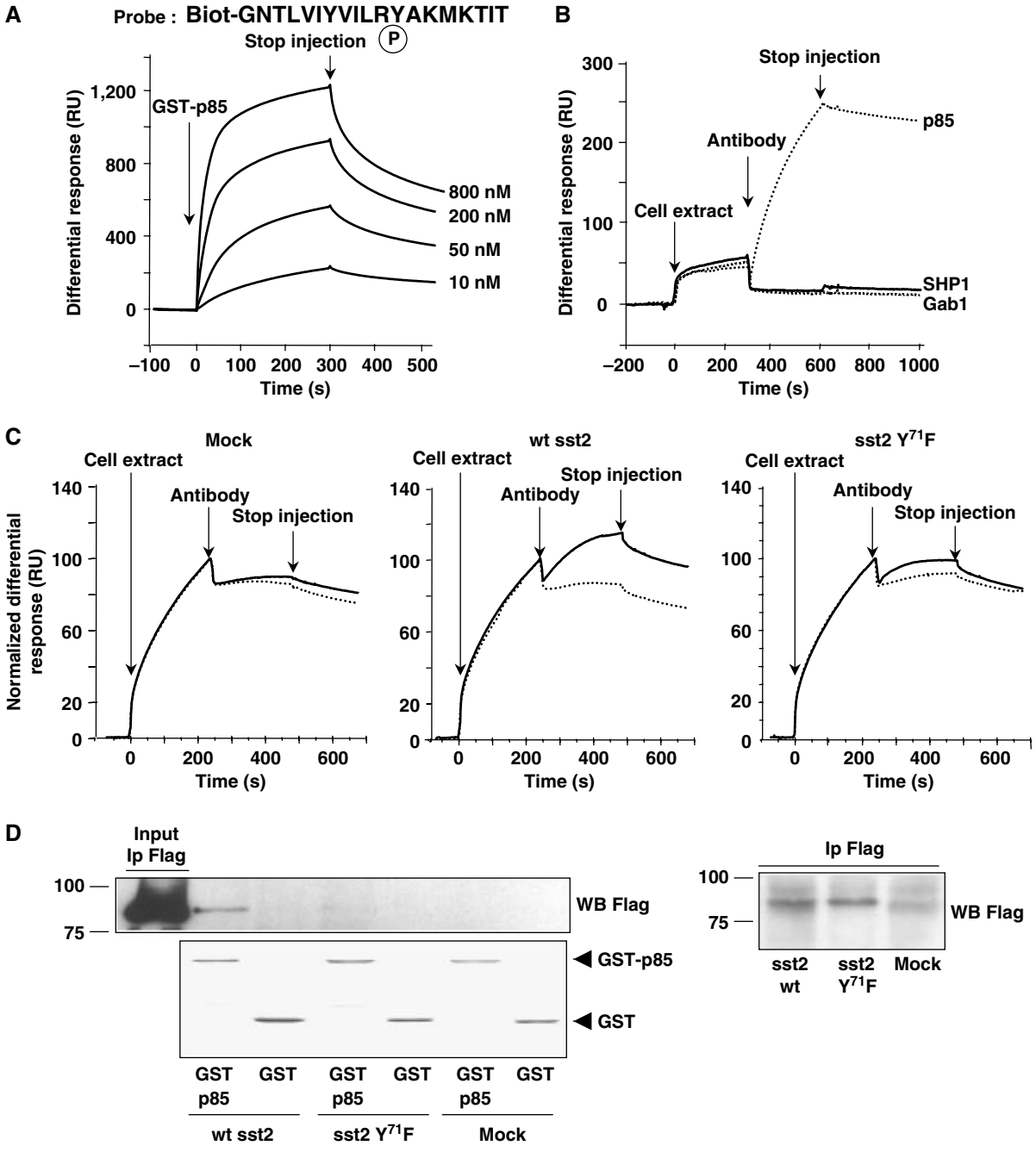

Figure 1 Identification and characterization of a direct interaction between sst2 and p85. (**A, B**) SPR analysis using two biotinylated peptides immobilized onto the Biacore chip, covering sst2-il$_1$ with the Y^{71} residue either phosphorylated or not, and injection of either (A) increasing concentrations of a recombinant GST-p85 protein, or (B) CHO cell extracts together with injection of anti-p85, -SHP-1 or Gab-1 antibody. Results are expressed as a differential response (RU quantified on the phosphorylated- versus nonphosphorylated-Y^{71}-peptide-containing flow cell). (**C**) SPR analysis using the recombinant GST-p85 protein immobilized onto the Biacore chip, and injection of either mock- (left panel), wild-type (middle panel) or mutated Y^{71}F flag-tagged sst2-transfected cell extracts (right panel). A competitive concentration of the sst2 phosphorylated-Y^{71}-containing peptide was coinjected (dotted line) or not (plain line) with the cell extracts. When indicated, the anti-flag antibody was injected. Results are expressed as a normalized differential response (RU), 100% referring to the maximal response observed for each cell extract in the absence of competitor peptide or antibody. (**D**) GST-pull-down assay using GST or GST-p85, coupled to glutathione agarose-beads, incubated with either mock-, wild-type or mutated Y^{71}F flag-tagged, sst2-transfected cell extracts. The presence of sst2 in the putative sst2–p85 complex was assessed by using the anti-flag antibody (left panel, upper). The total input of the wild-type sst2 protein present in the wild-type, flag-tagged, sst2-transfected cell extracts is visualized in lane 1 (Input). Equal levels of recombinant GST protein present in each lane were assessed by Coomassie blue staining of the gel (left panel, lower). Cell transfection efficiencies of both flag-tagged wild-type or mutated Y^{71}F sst2 were checked in the cell extracts used for the pull-down assay by immunoprecipitation/Western blot using the anti-flag antibody (right panel). Results presented in Figure 1 are representative of three independent experiments.

of the sst2 agonist RC-160), p85 co-immunoprecipitates with wild-type, but not specifically with mutated Y^{71}F sst2 (Figure 2A), nor with sst3, another member of the somatostatin receptor family which does not comprise the consensus YXXM motif (Figure 2B). This result, therefore, confirmed the involvement of the sst2-Y^{71} residue in the sst2–p85 inter-

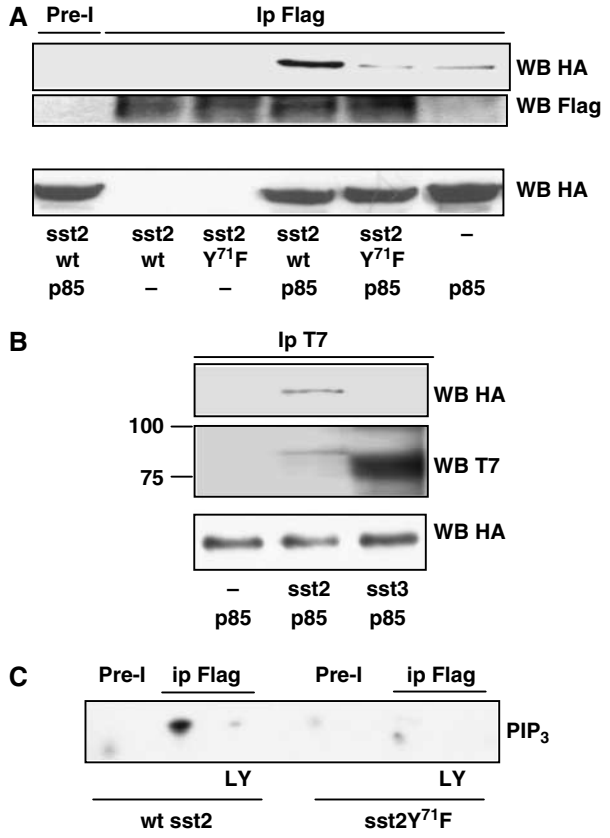

Figure 2 COS-7 cells. p85 and sst2, but not sst3, co-immunoprecipitate. COS-7 cells were transfected with HA-tagged p85 together with wild-type or mutated $Y^{71}F$ flag-tagged sst2 (**A, C**), or with T7-tagged sst2 or sst3 (**B**). (A, B) Immunoprecipitations were performed with the anti-flag (A) or anti-T7 (B) antibody, or preimmune (Pre-I) serum as control, which was followed by a western-blot using the anti-HA antibody (upper panels), or the anti-flag (A) or anti-T7 (B) antibody (middle panels) to check for equal levels of both transfection and immunoprecipitation of sst2/sst3 in each lane. Equal level of HA-p85 transfection was assessed by direct Western blot with the anti-HA antibody on a separate gel loaded with the same cell extracts (lower panels). (**C**) Measure of sst2-associated PI3K activity in COS-7 cell extracts transfected with wild-type or mutated $Y^{71}F$ flag-tagged sst2 (derived from lanes 2 and 3 of Figure 2A, respectively) immunoprecipitated with the anti-flag antibody, or preimmune (Pre-I) serum. When indicated, cell extracts were pretreated with 5 μM of LY294002. Results presented in Figure 2 are representative of three independent experiments.

action. Such sst2–p85 interaction was also observed in basal conditions in two other cell models expressing p85, CHO cells stably transfected with sst2 (CHO/sst2) and rat pancreatic cancer AR4-2J cells which express endogenous sst2 (Ferjoux *et al*, 2003). In these two models, p85 was present in the anti-sst2, but not preimmune serum, immunoprecipitate (Figures 3A and 4A, lanes 1 and 2, respectively).

Several reports have demonstrated the presence of an autoinhibitory motif in p85, which negatively regulates p110 catalytic activity. This p85 autoinhibitory action is relieved by both the engagement of either p85 SH2 domain to a phosphorylated-Y residue (Chan *et al*, 2002), and the phosphorylation of p85-Y^{688} residue, included in p85-SH2c (Cuevas *et al*, 2001), resulting in PI3K activation. Several arguments indicate that p85 autoinhibitory activity was relieved in our COS-7 and CHO cell models under basal conditions. Firstly, when assessing whether an endogenous PI3K activity associates with sst2, a PI3K activity was observed both in the anti-flag immunoprecipitate derived from wild-type, flag-tagged, sst2-transfected COS-7 cell extract (Figure 2C), or in the anti-sst2 immunoprecipitate from CHO/sst2 cells (Figure 3B, lane 1). This activity was specific because it was abrogated by addition of the PI3K inhibitor LY294002 (Figure 2C) and contributed to about 5% of the total PI3K activity (as measured in an anti-p85 immunoprecipitate, not shown). Interestingly, a robust total PI3K activity was observed in p85 immunoprecipitate from CHO/sst2 cells under basal conditions (Figure 3C, lane 1). We therefore suggest that, in the absence of added somatostatin and in the presence of serum, by binding p85, sst2 is permissive, rather than inhibitory, for growth factor-induced PI3K activity.

Somatostatin regulates sst2–p85 interaction and inhibits PI3K activity

To assess whether the sst2–p85 interaction is regulated by the somatostatin analog RC-160, the heterologous and endogenously sst2-expressing CHO/sst2 and AR4-2J cell models, respectively, were treated with 1 nM RC-160 in the presence of serum (Figures 3A and 4A). Treatment with RC-160 resulted in a time-dependent dissociation of p85 from sst2, which was maximal at 3–5 min.

Interestingly, we then demonstrated in CHO/sst2 cells that ligand-activated sst2 time-dependently inhibited both sst2-associated and total PI3K activities (Figure 3B and C), with a maximum at 3–5 min. Strikingly, RC-160-induced dissociation of p85 from sst2, rather than decreased p85 protein expression (which was stable during somatostatin treatment, not shown), was shown to be critical for somatostatin-mediated inhibition of total PI3K activity. Indeed, CHO cells expressing the mutated $Y^{71}F$-sst2 receptor, which does not bind p85, did not show RC-160-dependent inhibition of PI3K at both 3 and 5 min of treatment, as opposed to wild-type sst2-expressing CHO cells (Figure 3D). Functionality of the mutated $Y^{71}F$ sst2, in terms of appropriate folding and coupling to protein G, was confirmed (measure of inositol phosphate production, not shown) (Chen *et al*, 1997). Because about 5% of the total PI3K activity was estimated to bind the sst2 receptor, we hypothesize that, in a dynamic process, a large amount of the cellular p85-PI3K pool can be catalytically served via the sst2 interaction to be inactivated.

Accordingly, we have here unraveled an additional level of somatostatin-dependent PI3K inactivation through p85 tyrosine dephosphorylation. AR4-2J cell treatment with RC-160 reduced p85 tyrosine phosphorylation with a maximun at 3–5 min (Figure 4B). RC-160-mediated tyrosine dephosphorylation of p85 was observed in CHO/sst2 cells as well (not shown), this dephosphorylation occurring with a kinetic similar as that observed for RC-160-mediated inhibition of PI3K activity (Figure 3C). We hypothesize that tyrosine phosphatases including SHP-1 and/or SHP-2, which are activated by sst2 (Ferjoux *et al*, 2003), might be involved in p85 tyrosine dephosphorylation, as already described for SHP-1 (Cuevas *et al*, 1999).

Somatostatin inhibits sst2 tyrosine phosphorylation on the Y^{71} residue

We have previously demonstrated that sst2 is tyrosine-phosphorylated in the presence of serum, and that CHO/sst2 cell treatment with RC-160 inhibits this phosphorylation (Ferjoux

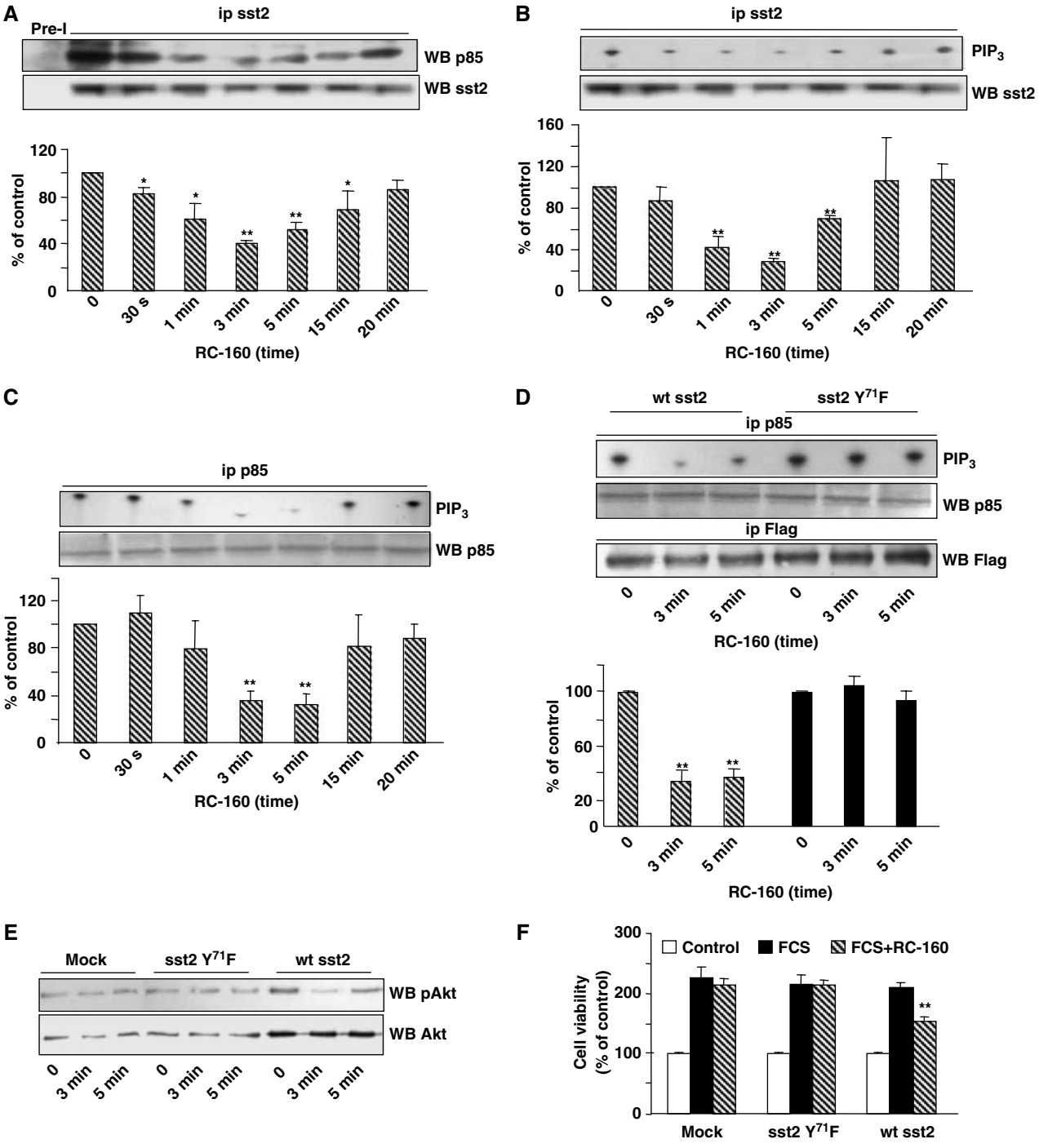

Figure 3 CHO cells. Somatostatin analog regulates sst2–p85 interaction and inhibits PI3K pathway and cell survival in a pY^{71}-dependent manner. CHO/sst2 cells (**A–C**) or CHO cells transfected with wild-type or mutated $Y^{71}F$ flag-tagged sst2 (**D–F**) were treated as indicated with RC-160. (A) Sst2–p85 interaction was assessed in sst2-, or in preimmune (Pre-I) serum as control, immunoprecipitates, by Western blot with the anti-p85 antibody. Equal level of immunoprecipitation in each lane was checked by immunoblotting the same membrane with the anti-sst2 antibody. Quantification of the sst2–p85 interaction was performed by densitometric analysis of the p85 immunoblot. Results are the means ± s.e.m. ($n = 3$) and expressed as 100% of the control RC-160-untreated cells. (B–D) Sst2-associated (B) or total (C, D) PI3K activities were assessed in sst2-, or p85 immunoprecipitates, respectively. Equal level of immunoprecipitation in each lane was checked by immunoblotting an additional gel loaded with the same immunoprecipitates either with the anti-sst2 antibody (B) or the anti-p85 antibody (C, D). Quantification of the PI3K activity was performed by densitometric analysis of the PIP_3 autoradiography. Results are the means ± s.e.m. ($n = 3$) and expressed as 100% of the control RC-160-untreated cells. (E) Immunoblot of Akt S^{473} phosphorylation. Equal loading of cell extract in each lane was checked by immunoblotting the same membrane with the anti-Akt antibody. (F) Cell viability assay using the MTT test in starved cells (control), serum-treated cells (FCS) or serum and RC-160-treated cells (FCS + RC-160, 10^{-9} M) for 24 h, as indicated. Results are the means ± s.e.m. of three independent experiments and expressed as 100% of control. Cell transfection efficiencies of both wild-type or mutated $Y^{71}F$ flag-tagged sst2 were checked in the same cell extracts by immunoprecipitation/Western blot using the anti-flag antibody (D, lower panel) (*$P < 0.05$ and **$P < 0.01$ for RC-160-treated CHO/sst2 cells versus serum-treated cells).

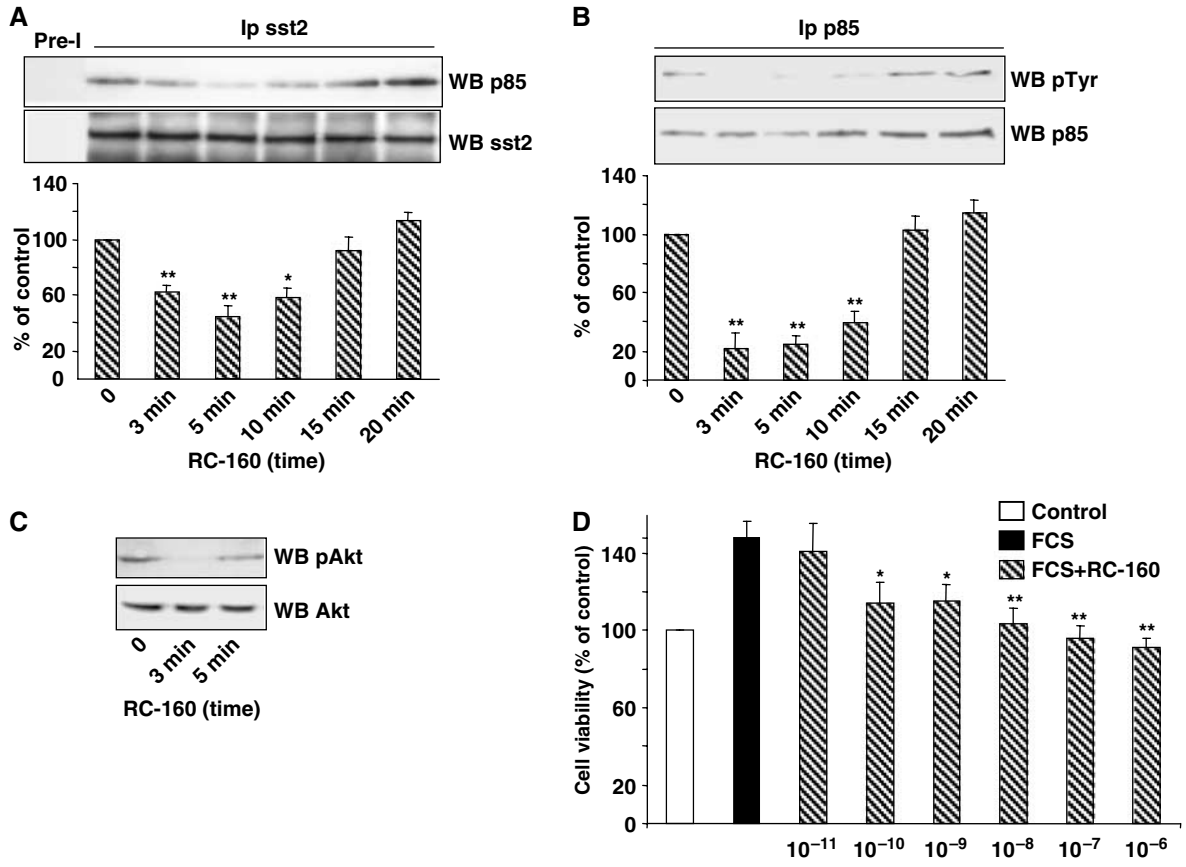

Figure 4 AR4-2J cells. Somatostatin analog regulates sst2–p85 interaction and inhibits PI3K pathway and cell survival. AR4-2J cells were treated as indicated with RC-160. (**A**) Sst2–p85 interaction was assessed in sst2-, or in preimmune (Pre-I) serum as control, immunoprecipitates, by Western blot with the anti-p85 antibody. Equal level of immunoprecipitation in each lane was checked by immunoblotting the same membrane with the anti-sst2 antibody. Quantification of the sst2–p85 interaction was performed by densitometric analysis of the p85 immunoblot. Results are the means ± s.e.m. ($n = 3$) and expressed as 100% of the control RC-160-untreated cells. (**B**) p85 tyrosine phosphorylation was assessed in p85 immunoprecipitates using an antiphosphotyrosine antibody. Equal level of immunoprecipitation in each lane was checked by immunoblotting the same membrane with the anti-p85 antibody. Quantification of p85 tyrosine phosphorylation was performed by densitometric analysis of the p-Tyr immunoblot. Results are the means ± s.e.m. ($n = 3$) and expressed as 100% of the control RC-160-untreated cells. (**C**) Immunoblot of Akt S^{473} phosphorylation. Equal loading of cell extract in each lane was checked by immunoblotting the same membrane with the anti-Akt antibody. (**D**) Cell viability assay using the MTT test in starved (control), serum-treated (FCS) or serum and RC-160-treated cells (FCS + RC-160, 10^{-11}–10^{-7} M) for 24 h, as indicated. Results are the means ± s.e.m. of three independent experiments and expressed as 100% of control (*$P < 0.05$ and **$P < 0.01$ for RC-160-treated AR4-2J cells versus serum-treated cells).

et al, 2003). We therefore investigated whether the specific residue Y^{71} in sst2-il_1 is tyrosine-phosphorylated and whether RC-160 regulates this phosphorylation. For this purpose, the specificity towards the sst2-il_1-pY^{71}-peptide of a phospho-(Tyr) p85 PI3K antibody (Li *et al*, 2003), which recognizes peptides and proteins containing phosphorylated tyrosine at the consensus YXXM motif, was tested using SPR (Figure 5A). This antibody was shown to specifically interact with the sst2-il_1-pY^{71}-peptide immobilized on the chip, but not with the corresponding unphosphorylated sst2-il_1-Y^{71}-peptide nor with an alternate tyrosine-phosphorylated pY^{312}-peptide encompassing the COOH-terminal 304–321 amino acids of sst2 sequence. Accordingly, the YXXM motif is present only in the first intracellular loop of the sst2 sequence. We therefore performed Western blotting experiments using this antibody to explore the phosphorylated status of the sst2 Y^{71} residue. Using anti-flag immunoprecipitates of COS cells either transfected with the wild-type or mutated Y^{71}F flag-tagged sst2 and cultured in the presence of serum, the phosphorylation of the Y^{71} residue was observed in the wild-type, but not specifically in the mutated Y^{71}, sst2. Interestingly, RC-160 decreased this phosphorylation after 5 min of cell treatment (Figure 5B). This result was confirmed in the endogenously sst2-expressing AR4-2J cells, whereby sst2 immunoprecipitates showed Y^{71} phosphorylation which was time-dependently decreased by RC-160 cell treatment (Figure 5C) with a kinetic similar as that observed for RC-160-mediated dissociation of p85 from sst2 (Figure 4A). We therefore hypothesize that the RC-160-mediated sst2/p85 dissociation resulted from sst2 tyrosine dephosphorylation on the Y^{71} residue. Interestingly, morphine, through activation of the μ-opioïd receptor, was shown to induce insulin signaling desensitization in a similar manner, through reduced tyrosine phosphorylation of the IRS-1 p85-binding site, consequently weakening IRS-1-p85 association (Li *et al*, 2003).

Sst2 inhibits the PI3K pathway and cell survival

To explore the physiological relevance for inhibition of the cell survival PI3K activity by somatostatin-activated sst2, phosphorylation on S^{473} of the PI3K target Akt and cell survival were assessed in CHO/sst2 and AR4-2J cells. Akt

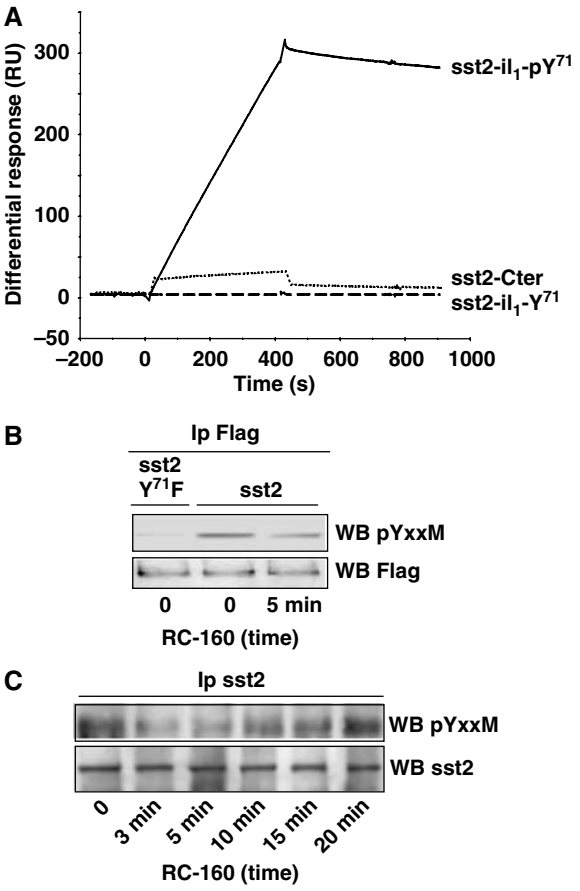

Figure 5 The sst2 Y^{71} residue is phosphorylated and somatostatin analog inhibits this phosphorylation. (**A**) Characterization of the phospho-(Tyr) p85 PI3K antibody. SPR analysis using three biotinylated peptides immobilized onto the Biacore chip, covering either sst2-il_1 with the Y^{71} residue phosphorylated or not (sst2-il_1-pY^{71} and sst2-il_1-Y^{71}, respectively), or sst2 C-terminal domain (amino acids 304–321) comprising of phosphorylated Y^{312} residue, and injection of the phospho-(Tyr) p85 PI3K antibody (pYXXM). Results are expressed as a differential response (RU quantified on the phosphorylated- versus nonphosphorylated-Y^{71}-peptide-containing flow cell). (**B**) Immunoblot using the phospho-(Tyr) p85 PI3K antibody (pYXXM) in anti-flag immunoprecipitates of COS-7 cells transfected with either wild-type or mutated Y^{71}F flag-tagged sst2, and treated or not with 10^{-9} M RC-160 for 5 min. Equal loading of cell extract in each lane was checked by immunoblotting the same membrane with the anti-flag antibody. (**C**) Immunoblot using the phospho-(Tyr) p85 PI3K antibody (pYXXM) in anti-sst2 immunoprecipitates of AR4-2J treated or not with 10^{-9} M RC-160, as indicated. Equal loading of cell extract in each lane was checked by immunoblotting the same membrane with the anti-sst2 antibody. These results are representative of three independent experiments.

S^{473} phosphorylation was indeed decreased at 3–5 min of RC-160 cell treatment in CHO/sst2 and AR4-2J cells (Figures 3E and 4C, respectively). This was associated with a RC-160-mediated inhibition of cell survival after 24 h of cell treatment (Figures 3F and 4D).

Excess activation of the PI3K pathway has been reported to be involved in pancreatic cancer cell invasive properties and resistance to chemotherapy (Ng *et al*, 2000; Stoll *et al*, 2005). The human pancreatic cancer BxPC-3 cells, whereby basal PI3K is robustly activated (Asano *et al*, 2004), have therefore been used to assess the relevance of the sst2–p85 interaction in sst2-mediated inhibition of tumor growth *in vivo*. Expressing sst2 in the BxPC-3 cells, which do not express endogenously this receptor, resulted in an autocrine loop whereby sst2 induced somatostatin expression, which, in turn, constitutively activated sst2 (Delesque *et al*, 1997). As a consequence, sst2-expressing BxPC-3 cell survival, tumor growth and metastasis were inhibited (Vernejoul *et al*, 2002; Guillermet *et al*, 2003).

Here, we showed that inhibition of cell survival of sst2-expressing BxPC-3 cells correlated with decreased PI3K activity and S^{473} phosphorylation of Akt (Figure 6A and B). Strikingly, specific inhibition of PI3K activity using up to 25 μM of LY294002 dose-dependently decreased survival of mock but not of sst2-expressing BxPC-3 cells (Figure 6C). Conversely, upregulating PI3K activity by transfecting sst2-expressing cells with the p110 constitutively active form (p110-CAAX) (Klippel *et al*, 1996) increased survival of these cells (Figure 6D). These results indicated that sst2-mediated inhibition of PI3K activity in BxPC-3 cells correlates with decreased cell survival.

Sst2-Y^{71} residue is critical for sst2-induced inhibition of the PI3K pathway

To assess the relevance of the pY^{71}-mediated sst2–p85 interaction in sst2-induced PI3K inhibition and subsequent inhibition of cell survival, CHO cells were transfected with wild-type or mutated Y^{71}F sst2. Mutating Y^{71} to F abrogated sst2-mediated inhibition of PI3K, S^{473} Akt phosphorylation and cell survival in CHO cells treated with RC-160 (Figure 3D–F).

In addition, BxPC-3 were stably transfected with either the empty vector (mock, clones M1 and M2) or wild-type sst2 (clones S1 and S2) or mutated Y^{71}F sst2 (clones Y1 and Y2), in order to follow the growth of the corresponding BxPC-3 cell xenografts in nude mice. Appropriate expression and localization to the cell membrane of wild-type or mutated Y^{71}F sst2 was controlled in each clone (Figure 7A). Interestingly, mutating Y^{71} to F resulted in abrogation of sst2-mediated inhibition of both PI3K and its targets Akt and NF-κB. A robust decreased PI3K activity was observed in S1 and S2, but not in Y1 and Y2 whose PI3K activities were comparable to those observed in M1 and M2 (Figure 7B). Decreased Akt S^{473} phosphorylation as well as NF-κB transcriptional activity were also observed in S1 and S2, but not in Y1 and Y2, as compared to M1 and M2 (Figure 7C and D).

Sst3 mediates somatostatin inhibitory effect on cell survival by a p53-dependent mechanism (Sharma *et al*, 1996). To explore the role of the PI3K pathway in this effect, BxPC-3 were stably transfected with either the empty vector (mock) or wild-type sst3 (Supplementary Figure 3A) and treated with somatostatin-14, which, as opposed to RC-160, has a high affinity for sst3 (Bousquet *et al*, 2004). As expected, somatostatin-14 abrogated serum-stimulated cell survival of sst3-, but not of mock-, expressing BxPC-3 cells with a maximal effect at 1 nM of somatostatin (Supplementary Figure 3C). However, Akt S^{473} phosphorylation was not affected by somatostatin-14 treatment either in sst3- or mock-expressing BxPC-3 cells (Supplementary Figure 3B).

All together, these results demonstrate that the presence of the sst2-il_1 sequence including the phosphorylated Y^{71} residue is critical not only for allowing direct interaction of p85 with sst2 but also for somatostatin-mediated inhibition of both PI3K pathway and cell survival. This conclusion is strengthened by our findings that somatostatin-mediated

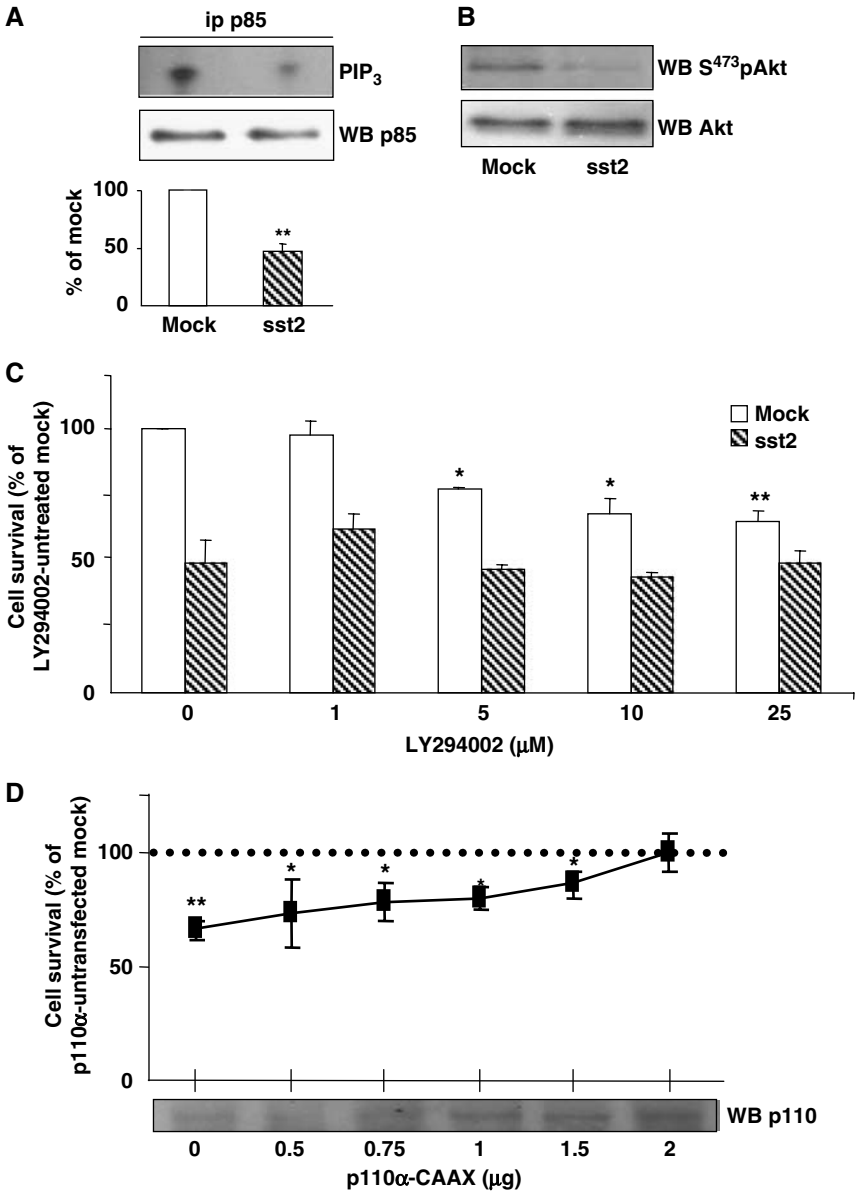

Figure 6 BxPC-3 cells. Sst2 inhibits PI3K activity and cell survival. (**A**) Total PI3K activity was assessed in p85 immunoprecipitates from mock- or sst2-expressing BxPC-3 cells. Equal level of immunoprecipitation in each lane was checked by immunoblotting an additional gel loaded with the same immunoprecipitates with the anti-p85 antibody. Quantification of the PI3K activity was performed by densitometric analysis of the PIP_3 autoradiography. Results are the means ± s.e.m. ($n = 3$) and expressed as 100% of mock BxPC-3 cells. $^{**}P < 0.01$ for sst2- versus mock-expressing BxPC-3 cells. (**B**) Immunoblot of Akt S^{473} phosphorylation of mock- or sst2-expressing BxPC-3 cells. Equal loading of cell extract in each lane was checked by immunoblotting the same membrane with the anti-Akt antibody. (**C, D**) Cell viability assay using the MTT test assessed on mock- or sst2-transfected BxPC-3 cells. BxPC-3 cells were treated with 0–25 μM of LY294002, and cell survival was expressed as 100% of mock LY294002-untreated BxPC-3 cells. Results are the means ± s.e.m. ($n = 3$). $^{*}P < 0.05$ and $^{**}P < 0.01$ for LY294002-treated versus control untreated BxPC-3 cells (C). sst2-expressing BxPC-3 cells were transfected with 0–2 μg of the constitutive active form of p110α (p110α-CAAX). Cell survival was expressed as 100% of p110α-untransfected (empty vector) mock BxPC-3 cells (as control). Transfection efficiency of p110α-CAAX was checked in a Western blot using the same cell extracts and an anti-p110 antibody. Results are the means ± s.e.m. ($n = 3$). $^{*}P < 0.05$ and $^{**}P < 0.01$ for p110α-CAAX-transfected sst2-expressing BxPC-3 cells versus p110α-untransfected mock BxPC-3 cells (D).

inhibition of cell survival was independent of PI3K pathway in cells expressing sst3, which does not present the YXXM consensus sequence and does not associate with p85 (Figure 2B).

Mutating sst2-Y^{71} to F reverted sst2-induced apoptosis and cell sensitization to TRAIL-induced apoptosis, and inhibition of cell tumorigenesis

To explore the relevance of the sst2–p85 interaction in sst2 tumor suppressor activity for pancreatic adenocarcinomas, apoptosis and cell survival were assessed in wild-type and mutated $Y^{71}F$ sst2-expressing cells. In S1 and S2, apoptosis was increased (Figure 7E), and cell survival decreased (Figure 7F), whereas no differences were observed between mock- and mutated $Y^{71}F$ sst2 clones. More interestingly, sst2-dependent sensitization to TRAIL (TNFα-related apoptosis inducing ligand) cytotoxic effect (Guillermet *et al*, 2003) was abrogated in Y1 and Y2 (Figure 7G). As expected, cell treatment with TRAIL decreased M1 and M2 cell survival, which was further decreased in S1 and S2 (sst2-dependent

cell sensitization). However, no cell sensitization to TRAIL was observed in Y1 and Y2, whose survival in the presence of TRAIL treatment was similar to M1 and M2. These results, therefore, indicated that sst2-Y^{71} residue is critical for sst2-induced apoptosis and cell sensitization to TRAIL-induced apoptosis.

Finally, wild-type and mutated Y^{71}F-sst2-expressing cells were injected into nude mice and the growth of resulting tumors was compared (Figure 7H). Whereas exponential growth was observed as soon as day 43 postinjection for M1 and M2 tumors, which reached a volume of 2000 mm^3 at day 61, sst2 effectively abrogated growth of S1 and S2 tumors (Delesque *et al*, 1997). Surprisingly, growth of Y1 and Y2 tumors was significantly accelerated as compared to S1 and S2 tumors, which indicated that the sst2-Y^{71} residue is critical for sst2 anti-tumorigenic action *in vivo*. However, although Y1 and Y2 tumors had an exponential growth starting at day 43 after cell injection as well, their volume reached approximately half of mock tumor volume at day 61. This result suggests that alternate sst2-induced antitumorigenic pathways, other than PI3K inhibition, are stimulated by the mutated sst2 receptor in these cells.

Regulation of the PI3K pathway through ligand-activated GPCRs has been demonstrated in several systems, and comprises transactivation or inhibition of growth factor-induced PI3K activation (Cui *et al*, 2002; Nair and Sealfon, 2003). However, these receptors do not contain the p85-binding YXXM motif, suggesting that this regulation is indirect, affecting the activity of proteins included in growth factor receptor signaling cascades. Identifying sst2 and p85 as direct interacting partners provide the first demonstration of a physical interaction between the p85 PI3K regulatory subunit and a GPCR. Interestingly, in a nonexhaustive database of GPCR (780 entries), the YXXM motif is retrieved in the intracellular loop sequences of 40 GPCR, which are listed in Supplementary Table 1 (J Iacovoni, personal communication). The YXXM motif is present for example in the il_1 of somatostatin receptors sst1, sst2 and sst4, and of some closely related somatostatin GPCR of the opioïd family, including μ, δ and κ. Strikingly, these receptors regulate PI3K activity, important for cell proliferation, cell survival, antinociception or receptor desensitization (Tan *et al*, 2003). Physical interaction with p85 might therefore constitute an original mechanism involved in such receptor-dependent regulation of PI3K.

In conclusion, in addition to demonstrating novel signaling for sst2 proapoptotic and antioncogenic actions in pancreatic cancer cells through inhibition of PI3K, these results present the first demonstration of a physical interaction occurring between the p85 PI3K regulatory subunit and a GPCR, sst2. Inhibition of PI3K activity through somatostatin-dependent disruption of the p85–sst2 complex reveals a novel original mechanism for limiting PI3K activity. These results also provide new insights regarding molecular pathways facilitating cooperativity or inhibitory crosstalk between growth factor-activated PI3K-dependent survival pathways and GPCR signaling, which may be of critical interest for novel antineoplastic therapy.

Materials and methods

Antibodies

Polyclonal antibody directed against p85 was from Upstate Biotechnology; Akt, S^{473}-phosphoAkt and phospho-(Tyr) p85 PI3K-binding motif from Cell Signaling; p110 from Santa-Cruz and sst2 receptor antibodies were either a generous gift from S Schulz or generated in our laboratory (Ferjoux *et al*, 2003). Monoclonal antibody directed against hemagglutinin (HA, 12CA5) was from Roche Diagnostics; M2 Flag from Sigma and anti-phosphotyrosine 4G10 from Upstate Biotechnology.

Cell culture and transfections

CHO (DG44 variant) and human pancreatic cancer BxPC-3 cells have previously been transfected either with the human 1.35-kbp sst2 cDNA or with mock vector, and characterized (Delesque *et al*, 1997; Ferjoux *et al*, 2003). COS-7, CHO, AR4-2J-B13, BxPC-3 and COS-7 cells were cultured as described (Shen *et al*, 2000; Ferjoux *et al*, 2003; Guillermet *et al*, 2003). BxPC-3 cells were stably transfected with either the human wild-type or mutated Y^{71}F sst2 or sst3 cDNA and clones were selected using 400 μg/ml of geneticin. When indicated, cells were treated with the somatostatin analog RC-160 (generous gift from AV Schally) or with somatostatin-14 in the presence of fetal calf serum (FCS).

Flag-tagged wild-type or mutant Y^{71}F sst2 receptor and/or HA-tagged p85 cDNAs were transiently transfected into COS-7 cells by using DEAE/dextran, or in CHO cells by using FuGENE6 (Roche Diagnostics).

Immunoprecipitation and Western blot

Immunoprecipitation and Western blot were performed as previously described (Ferjoux *et al*, 2003). CHAPS (1.5%) was used as detergent. Samples were separated on 7.5% SDS–PAGE. Immunodetection was performed using horseradish peroxidase-conjugated anti-mouse or anti-rabbit IgG followed by ECL (Pierce Chemical).

Site-directed mutagenesis

Mutations of sst2-Y^{71}F residue and of p85 E^{635}L, R649 M, E^{666}L and D^{708}A residues were performed using site-directed mutagenesis (Stratagene).

GST pull-down assays

GST-fusion proteins containing the wild-type or mutated sequences of p85 were expressed and isolated (Ferjoux *et al*, 2003). For pull-down experiments, 1 mg of COS-7 cell extracts transfected or not with wild-type or Y^{71}F sst2 were incubated with the GST or GST-p85 protein overnight at 4°C. Complexes were then collected and subjected to SDS–PAGE using the anti-flag antibody.

SPR

Real-time binding experiments were performed with a BIAcore 3000 biosensor instrument (BIAcore AB) and quantified in terms of resonance units (RU) (1000 RU = 1 ng of protein bound/mm^2 of flow cell surface) (Ferjoux *et al*, 2003). Synthetic biotinylated peptides covering sst2-il_1 (from residues T^{62} to T^{78}) or COOH-terminal domain (from residues N^{304} to K^{321} with Y^{312} phosphorylated) (Neosystem) were immobilized onto streptavidin-coated carboxymethylated dextran chips (BIAcore AB). Two flow cells were coated with 50 RU of either the phosphorylated- (flow cell 2) or non-phosphorylated-Y^{71} peptide (flow cell 1). Sensograms were analyzed as the differential response between binding on the phosphorylated- versus nonphosphorylated-Y^{71}-peptide. Wild-type or mutated GST-p85 fusion proteins were injected in the running buffer (HEPES 10 mM, NaCl 150 mM, EDTA 3 mM, polysorbate 0.005%). Kinetic constants (K_{on}, K_{off}, K_D) were evaluated using BIAevaluation 4.01 software (BIAcore AB). The phospho-(Tyr) p85 PI3K-binding motif antibody was injected at 1% in the running buffer. Fusion GST-p85 proteins were immobilized on a carboxymethylated dextran chip (chip CM5, BIAcore AB). Fusion protein (7200 RU) was crosslinked on flow cell 2, whereas flow cell 1 was activated and deactivated as a nonspecific interaction reference. Cell extracts (100–400 μg/ml) were first injected on both flow cells 1 and 2, and antibodies were then coinjected (1–3% v/v). For competition experiment, 7 μM of the phosphorylated-Y^{71}-peptide was injected together with the cell extracts.

For further analysis of the proteins bound onto the phosphorylated-Y^{71}-peptide using MALDI-TOF MS, 250 RU of peptide was immobilized on 3 flow cells. The equivalent of 2000 RU of bound proteins, issued from the injection of p85-tranfected CHO cell extract, was eluted using the microrecovery procedure (Martinez *et al*, 2003).

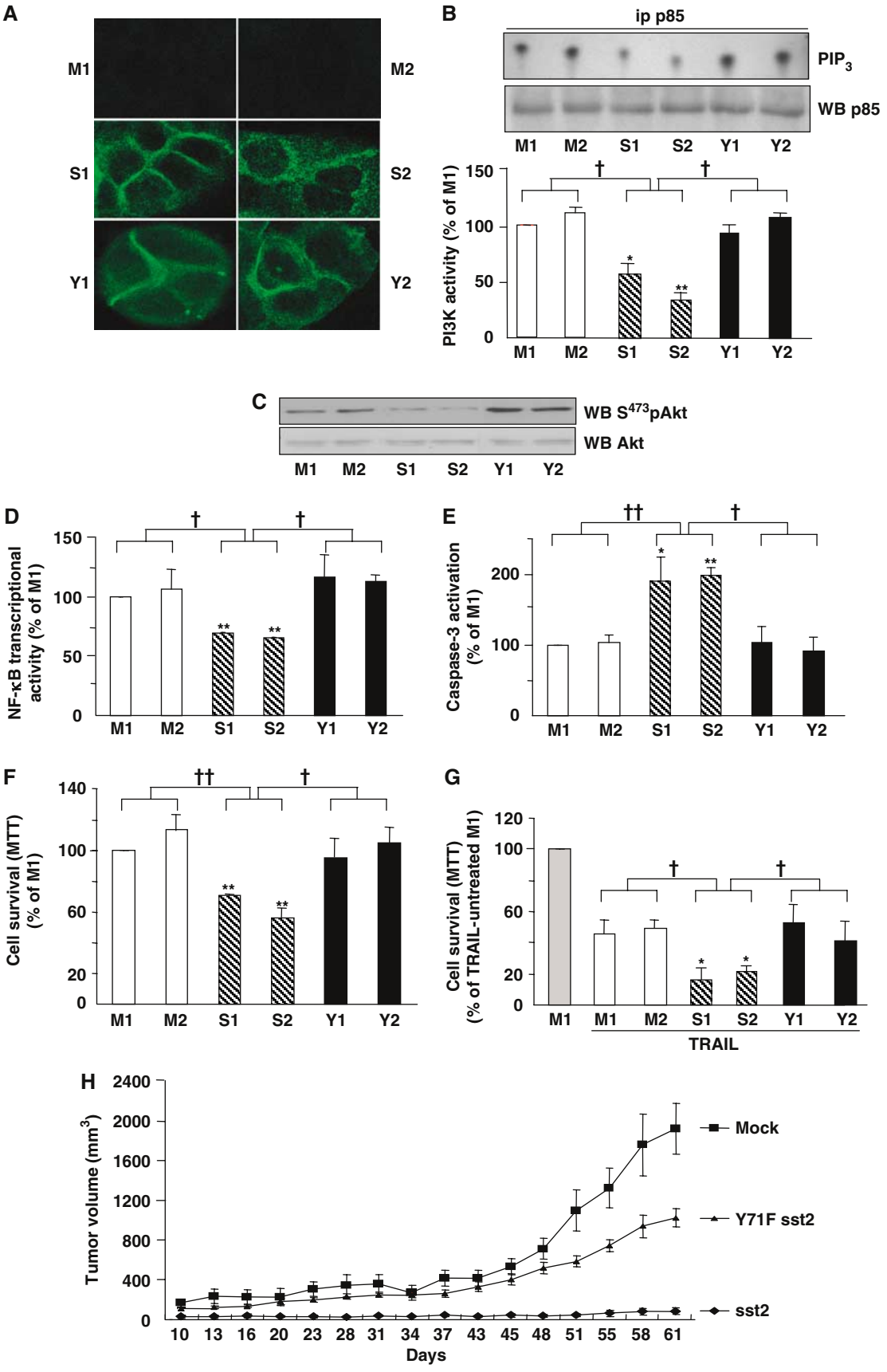

Molecular modeling

sst2-il$_1$, flanked with its transmembrane domains (TM) I and II (residues 42–105), was constructed by homology modeling using the rhodopsin crystal structure as template (Teller *et al*, 2001). The crystal structure of the COOH-terminal SH2 domain of p85 (SH2c), complexed with a tyrosine-phosphopeptide from the PDGF receptor,

Figure 7 BxPC-3 cells. Sst2-Y^{71} residue is critical for sst2-induced inhibition of PI3K activity, cell survival and cell tumorigenicity *in vivo*. (**A**) Immunocytochemistry and confocal microscopy of sst2 expression in mock M1 and M2, sst2-expressing S1 and S2, and mutated $Y^{71}F$ sst2-expressing BxPC-3 clones using the polyclonal anti-sst2 antibody. (**B**) Total PI3K activity was assessed in p85 immunoprecipitates from M1, M2, S1, S2, Y1 and Y2 clones. Equal level of immunoprecipitation in each lane was checked by immunoblotting an additional gel loaded with the same immunoprecipitates with the anti-p85 antibody. Quantification of the PI3K activity was performed by densitometric analysis of the PIP_3 autoradiography. Results are the means ± s.e.m. ($n = 3$) and expressed as 100% of M1. (**C**) Immunoblot of Akt S^{473} phosphorylation of M1, M2, S1, S2, Y1 and Y2 clones. Equal loading of cell extract in each lane was checked by immunoblotting the same membrane with the anti-Akt antibody. (**D**) NF-κB transcriptional activity was assessed in M1, M2, S1, S2, Y1 and Y2 clones after transfection of a luciferase reporter vector containing or not (control) four tandem copies of the NF-κB consensus sequence κB. Normalized luciferase activities were expressed as 100% of M1. Results are the means ± s.e.m. ($n = 3$). (**E**) Caspase-3 activity was assessed by flow cytometry in M1, M2, S1, S2, Y1 and Y2 clones, and expressed as 100% of M1. Results are the means ± s.e.m. ($n = 3$). (**F, G**) Cell viability assay using the MTT test assessed on M1, M2, S1, S2, Y1 and Y2 clones, untreated (F) or treated (G) with TRAIL (100 ng/ml) for 24 h, as indicated. Results are the means ± s.e.m. of three independent experiments and expressed as 100% of M1 (TRAIL-untreated) cells. $^{*}P < 0.05$ and $^{**}P < 0.01$ for M2, S1, S2, Y1 or Y2 versus M1. $^{\dagger}P < 0.05$ and $^{\dagger\dagger}P < 0.01$ for S1 and S2 versus M1 and M2 or versus Y1 and Y2. (**H**) Either mock (M1 and M2) or wild type (S1 and S2) or mutated Y^{71} sst2 (Y1 and Y2)-expressing clones were subcutaneously injected in *athymic* mice (eight per group), and tumor growth was monitored for up to 61 days. Results shown are the mean tumor volume ± s.e.m. ($n = 3$).

was as well used as template (Pauptit *et al*, 2001). The docking of the sst2-il_1/p85-SH2c complex was achieved by manual refinement, using electrostatic interactions. Procedures of minimizations were then applied to the sst2-il_1/p85-SH2c complex, using Insight II modules (Homology, Discover and biopolymer, Accelrys).

Phosphatidylinositol 3-kinase assay

PtdIns-3-kinase activity was measured in anti-sst2 or anti-p85 immunoprecipitates (Daulhac *et al*, 1999). Phospholipids were analyzed by thin-layer chromatography and autoradiography.

Flow cytometry for caspase-3 activity

Cells were fixed using the Cytofix/Cytosperm™ solution and incubated with the antiactive caspase-3 antibody in the Perm/Wash solution (Becton Dickinson) for 30 min at 4°C. Flow cytometry analyses were performed on the Becton Dickinson FACSCalibur.

Cell viability assay

Mitochondrial viability was measured using the MTT (3-[4,5-dimethylthiazol-2-yl]-2,5-diphenyl tetrazolium bromide) (Sigma) colorimetric assay (Guillermet *et al*, 2003).

Luciferase reporter assay

Cells were transfected with a mixture of NF-κB-Luc or control pTAL vector (Clontech) + pCMVβGal vector using Polyethylenimine (Upstate Biotechnology). Luciferase activity was measured using a Labsystems Luminoskan 96-well plate luminometer (Thermolab system), and β-galactosidase activity by spectrophotometry (MRX Dynex Technologies), after addition of the respective substrates. Luciferase activity was first normalized for each point with the respective β-galactosidase activity, and then with the luciferase activity measured in the respective pTAL-transfected cells.

Athymic mice xenograft

10^7 BxPC-3 cells expressing or not the wild-type or $Y^{71}F$ sst2 receptor were inoculated s.c. into athymic female mice (Swiss nude/nude) of 8 weeks of age that were maintained in pathogen-free conditions. Tumor dimensions were measured every 3–6 days and the corresponding volumes were estimated by the equation: $V = W^2 \times L/2$, where W = width (mm) and L = length of tumor (mm). Mice were killed 9 weeks after cell inoculation.

Statistical analysis

Experiments were performed at least three times. Statistical analysis was performed by unpaired *t*-test. All values are mean ± s.e.m.

Supplementary data

Supplementary data are available at *The EMBO Journal* Online (http://www.embojournal.org).

Acknowledgements

We thank Dr P Raynal (INSERM U563, Toulouse, France) for providing p85 constructs, Dr S Schulz (Institut fur Pharmakologie und Toxikologie, Magdeburg, Germany) for providing the polyclonal sst2 antibody and the sst3 cDNA (Pfeiffer *et al*, 2001) and Dr AV Schally (Tulane University, New Orleans, LA) for providing the somatostatin analog RC-160. We also thank Dr Jason Iacovoni (INSERM U589, Toulouse, France) for his bioinformatic help screening the GPCR database for the YXXM motif. This work was supported by Association pour la Recherche Contre le Cancer (3219 and ARECA Proteomic and Cancer), Ligue Nationale Contre le Cancer (R04045BB and R04044BB), the European Community (QLG3-CT-1999-00908) and the Université Paul Sabatier of Toulouse (A01-2004). JG-G, EA-L and AF are recipients of a fellowship from the French government.

References

Asano T, Yao Y, Zhu J, Li D, Abbruzzese JL, Reddy SA (2004) The PI 3-kinase/Akt signaling pathway is activated due to aberrant Pten expression and targets transcription factors NF-kappaB and c-Myc in pancreatic cancer cells. *Oncogene* **23:** 8571–8580

Bousquet C, Guillermet J, Vernejoul F, Lahlou H, Buscail L, Susini C (2004) Somatostatin receptors and regulation of cell proliferation. *Dig Liver Dis* **36** (Suppl 1)**:** S2–S7

Buscail L, Saint-Laurent N, Chastre E, Vaillant JC, Gespach C, Capella G, Kalthoff H, Lluis F, Vaysse N, Susini C (1996) Loss of sst2 somatostatin receptor gene expression in human pancreatic and colorectal cancer. *Cancer Res* **56:** 1823–1827

Cantley LC (2002) The phosphoinositide 3-kinase pathway. *Science* **296:** 1655–1657

Chan TO, Rodeck U, Chan AM, Kimmelman AC, Rittenhouse SE, Panayotou G, Tsichlis PN (2002) Small GTPases and tyrosine kinases coregulate a molecular switch in the phosphoinositide 3-kinase regulatory subunit. *Cancer Cell* **1:** 181–191

Chen L, Fitzpatrick VD, Vandlen RL, Tashjian Jr AH (1997) Both overlapping and distinct signaling pathways for somatostatin receptor subtypes SSTR1 and SSTR2 in pituitary cells. *J Biol Chem* **272:** 18666–18672

Cuevas B, Lu Y, Watt S, Kumar R, Zhang J, Siminovitch KA, Mills GB (1999) SHP-1 regulates Lck-induced phosphatidylinositol 3-kinase phosphorylation and activity. *J Biol Chem* **274:** 27583–27589

Cuevas BD, Lu Y, Mao M, Zhang J, LaPushin R, Siminovitch K, Mills GB (2001) Tyrosine phosphorylation of p85 relieves its inhibitory activity on phosphatidylinositol 3-kinase. *J Biol Chem* **276:** 27455–27461

Cui TX, Nakagami H, Nahmias C, Shiuchi T, Takeda-Matsubara Y, Li JM, Wu L, Iwai M, Horiuchi M (2002) Angiotensin II subtype 2 receptor activation inhibits insulin-induced phosphoinositide 3-kinase and Akt and induces apoptosis in PC12W cells. *Mol Endocrinol* **16:** 2113–2123

Daulhac L, Kowalski-Chauvel A, Pradayrol L, Vaysse N, Seva C (1999) Src-family tyrosine kinases in activation of ERK-1 and p85/p110-phosphatidylinositol 3-kinase by G/CCKB receptors. *J Biol Chem* **274:** 20657–20663

Delesque N, Buscail L, Esteve JP, Saint-Laurent N, Muller C, Weckbecker G, Bruns C, Vaysse N, Susini C (1997) sst2 somatostatin receptor expression reverses tumorigenicity of human pancreatic cancer cells. *Cancer Res* **57:** 956–962

Ferjoux G, Lopez F, Esteve JP, Ferrand A, Vivier E, Vely F, Saint-Laurent N, Pradayrol L, Buscail L, Susini C (2003) Critical role of Src and SHP-2 in sst2 somatostatin receptor-mediated activation of SHP-1 and inhibition of cell proliferation. *Mol Biol Cell* **14:** 3911–3928

Foukas LC, Beeton CA, Jensen J, Phillips WA, Shepherd PR (2004) Regulation of phosphoinositide 3-kinase by its intrinsic serine kinase activity *in vivo*. *Mol Cell Biol* **24:** 966–975

Guillermet J, Saint-Laurent N, Rochaix P, Cuvillier O, Levade T, Schally AV, Pradayrol L, Buscail L, Susini C, Bousquet C (2003) Somatostatin receptor subtype 2 sensitizes human pancreatic cancer cells to death ligand-induced apoptosis. *Proc Natl Acad Sci USA* **100:** 155–160

Harrington LS, Findlay GM, Lamb RF (2005) Restraining PI3K: mTOR signalling goes back to the membrane. *Trends Biochem Sci* **30:** 35–42

Klippel A, Reinhard C, Kavanaugh WM, Apell G, Escobedo MA, Williams LT (1996) Membrane localization of phosphatidylinositol 3-kinase is sufficient to activate multiple signal-transducing kinase pathways. *Mol Cell Biol* **16:** 4117–4127

Kumar M, Liu ZR, Thapa L, Qin RY (2004) Anti-angiogenic effects of somatostatin receptor subtype 2 on human pancreatic cancer xenografts. *Carcinogenesis* **25:** 2075–2081

Kuriyan J, Cowburn D (1997) Modular peptide recognition domains in eukaryotic signaling. *Annu Rev Biophys Biomol Struct* **26:** 259–288

Leis H, Page A, Ramirez A, Bravo A, Segrelles C, Paramio J, Barettino D, Jorcano JL, Perez P (2004) Glucocorticoid receptor counteracts tumorigenic activity of Akt in skin through interference with the phosphatidylinositol 3-kinase signaling pathway. *Mol Endocrinol* **18:** 303–311

Li Y, Eitan S, Wu J, Evans CJ, Kieffer B, Sun X, Polakiewicz RD (2003) Morphine induces desensitization of insulin receptor signaling. *Mol Cell Biol* **23:** 6255–6266

Luo J, Manning BD, Cantley LC (2003) Targeting the PI3K-Akt pathway in human cancer: rationale and promise. *Cancer Cell* **4:** 257–262

Martinez LO, Jacquet S, Esteve JP, Rolland C, Cabezon E, Champagne E, Pineau T, Georgeaud V, Walker JE, Terce F, Collet X, Perret B, Barbaras R (2003) Ectopic beta-chain of ATP synthase is an apolipoprotein A-I receptor in hepatic HDL endocytosis. *Nature* **421:** 75–79

Nair VD, Sealfon SC (2003) Agonist-specific transactivation of phosphoinositide 3-kinase signaling pathway mediated by the dopamine D2 receptor. *J Biol Chem* **278:** 47053–47061

Ng SSW, Tsao MS, Chow S, Hedley DW (2000) Inhibition of phosphatidylinositide 3-kinase enhances gemcitabine-induced apoptosis in human pancreatic cancer cells. *Cancer Res* **60:** 5451–5455

Panayotou G, Gish G, End P, Truong O, Gout I, Dhand R, Fry MJ, Hiles I, Pawson T, Waterfield MD (1993) Interactions between SH2 domains and tyrosine-phosphorylated platelet-derived growth factor beta-receptor sequences: analysis of kinetic parameters by a novel biosensor-based approach. *Mol Cell Biol* **13:** 3567–3576

Pauptit RA, Dennis CA, Derbyshire DJ, Breeze AL, Weston SA, Rowsell S, Murshudov GN (2001) NMR trial models: experiences with the colicin immunity protein Im7 and the p85alpha C-terminal SH2-peptide complex. *Acta Crystallogr D Biol Crystallogr* **57:** 1397–1404

Pfeiffer M, Koch T, Schroder H, Klutzny M, Kirscht S, Kreienkamp HJ, Hollt V, Schulz S (2001) Homo- and heterodimerization of somatostatin receptor subtypes. Inactivation of sst(3) receptor function by heterodimerization with sst(2A). *J Biol Chem* **276:** 14027–14036

Sharma k, Patel YC, Srikant CB (1996) Subtype-selective induction of wild-type p53 and apoptosis, but not cell cycle arrest, by human somatostatin receptor 3. *Mol Endocrinol* **10:** 1688–1696

Shen CN, Slack JM, Tosh D (2000) Molecular basis of transdifferentiation of pancreas to liver. *Nat Cell Biol* **2:** 879–887

Simoncini T, Hafezi-Moghadam A, Brazil DP, Ley K, Chin WW, Liao JK (2000) Interaction of oestrogen receptor with the regulatory subunit of phosphatidylinositol-3-OH kinase. *Nature* **407:** 538–541

Stoll V, Calleja V, Vassaux G, Downward J, Lemoine NR (2005) Dominant negative inhibitors of signalling through the phosphoinositol 3-kinase pathway for gene therapy of pancreatic cancer. *Gut* **54:** 109–116

Takagi N, Sasakawa K, Besshoh S, Miyake-Takagi K, Takeo S (2003) Transient ischemia enhances tyrosine phosphorylation and binding of the NMDA receptor to the Src homology 2 domain of phosphatidylinositol 3-kinase in the rat hippocampus. *J Neurochem* **84:** 67–76

Tan M, Groszer M, Tan AM, Pandya A, Liu X, Xie CW (2003) Phosphoinositide 3-kinase cascade facilitates mu-opioid desensitization in sensory neurons by altering G-protein-effector interactions. *J Neurosci* **23:** 10292–10301

Teller DC, Okada T, Behnke CA, Palczewski K, Stenkamp RE (2001) Advances in determination of a high-resolution three-dimensional structure of rhodopsin, a model of G-protein-coupled receptors (GPCRs). *Biochemistry* **40:** 7761–7772

Vernejoul F, Faure P, Benali N, Calise D, Tiraby G, Pradayrol L, Susini C, Buscail L (2002) Antitumor effect of *in vivo* somatostatin receptor subtype 2 gene transfer in primary and metastatic pancreatic cancer models. *Cancer Res* **62:** 6124–6131

Vivanco I, Sawyers CL (2002) The phosphatidylinositol 3-kinase AKT pathway in human cancer. *Nat Rev Cancer* **2:** 489–501

Weckbecker G, Lewis I, Albert R, Schmid HA, Hoyer D, Bruns C (2003) Opportunities in somatostatin research: biological chemical and therapeutic aspects. *Nat Rev Drug Discov* **2:** 999–1017

Zhang SQ, Tsiaras WG, Araki T, Wen G, Minichiello L, Klein R, Neel BG (2002) Receptor-specific regulation of phosphatidylinositol 3′-kinase activation by the protein tyrosine phosphatase Shp2. *Mol Cell Biol* **22:** 4062–4072

